ISBN: 978-3-95450-208-0 doi:10.18429/JACoW-IPAC2019-TUYPLM3

STATUS OF THE MAX IV ACCELERATORS

P. F. Tavares*, E.Al-Dmour,Å.Andersson, J.Breunlin, F.Cullinan, E.Mansten, S.Molloy, D.Olsson, D.K.Olsson, M.Sjöström, S.Thorin
MAX IV Laboratory, Lund University, Lund, Sweden

Abstract

The MAX IV facility in Lund, Sweden, consists of three electron accelerators and their respective synchrotron radiation beamlines: a 3 GeV ring, which is the first implementation worldwide of a multi-bend achromat lattice, a 1.5 GeV ring optimized for soft X-Rays and UV radiation production and a 3 GeV linear accelerator that acts as a full-energy injector into both rings and provides electron pulses as short as 100 fs that produce X-rays by spontaneous emission in the undulators of the short-pulse facility (SPF). In this paper, we review the latest achieved accelerator performance and operational results.

INTRODUCTION

The MAX IV facility [1] consists of three electron accelerators and their respective synchrotron radiation beamlines. Two electron storage rings operate at different energies (1.5 GeV and 3 GeV) in order to cover a wide photon energy range in an optimized way with short-period insertion devices, whereas a linear accelerator serves as a full-energy injector into both rings and provides electron pulses as short as 100 fs that produce X-rays by spontaneous emission in the undulators of the short-pulse facility (SPF).

The 3 GeV ring [2] is optimized for the production of high-brightness X-rays and features a 20-fold seven-bend achromat lattice reaching a bare lattice emittance of 330 pm rad. Achieving such a low emittance in only 528 m of circumference requires a compact magnet design [3] and corresponding narrow gap NEG-coated vacuum chambers [4]. The reduced chamber dimensions lead in turn to an increased risk of collective instabilities, e.g. transverse multi-bunch instabilities driven by resistive wall impedance. Key ingredients to deal with those issues are the use of a relatively low main RF frequency (100 MHz) [5] and passively operated third-harmonic cavities [6] which lengthen the bunches, reduce the electron density and increase the incoherent synchrotron frequency spread, providing enhanced damping of coherent instabilities.

Details of early 3 GeV ring commissioning are given in [7,8] whereas initial optics commissioning is described in [9] and first year commissioning results are reported in [10]. Despite a number of somewhat unconventional features of the design, such as the use of compact magnet blocks, nearly fully NEG-coated small-aperture vacuum chambers, a 100 MHz RF system and a single kicker injection scheme with a full energy linac as injector, commissioning of the ring did not uncover any show-stoppers on the way to achieving baseline performance.

The nominal 500 mA stored current in multi-bunch mode and 9 mA in single-bunch mode have been demonstrated during machine studies. Routine delivery to beamlines is in top-up mode at 250 mA (limited by available RF power) with >90% injection efficiency using a multipole injection kicker, closed undulator gaps and open beamline shutters. The product of beam current and lifetime from gas scattering is larger than 20 A.h, confirming the excellent performance of the NEG coated system. The nominal horizontal electron beam emittance at low current has been demonstrated and vertical emittances around 8 pmrad are routinely delivered. An excellent orbit stability has been achieved with RMS motion (integrated from 0.1 up to 100 Hz) below 1.3% and 5.5 % of the RMS beam size in the horizontal and vertical directions respectively.

The 1.5 GeV ring profits by the same compact magnet design to achieve significantly lower emittance compared to its predecessor (MAX II) with roughly the same circumference. The nominal 500 mA stored beam current has been demonstrated and five insertion devices have been installed.

The MAX IV linac [11] routinely delivers beam to both storage rings for full energy injection and top-up with closed undulator gaps and open front-ends. In-between top-ups the mode is switched to high brightness mode for the SPF [12]. Switching is done using a state machine that keeps track of all setting for the different linac and ring configurations. To meet exactly the energy required for each ring and SPF, the fill-time to the energy doubling SLED [30] units is adjusted.

In the following sections, we report on recent development highlights in each of the MAX IV accelerators.

LINEAR ACCELERATOR

High Brightness Mode

The two magnetic double achromats used as bunch compressors [13] in the MAX IV linac have a positive R56 unlike the commonly used magnetic chicane which has a negative R56. The energy chirp needed for compression is done by accelerating the electrons on the falling slope of the RF voltage. The natural T566 of the compressors is positive and with the positive R56, this has a linearising effect on the longitudinal phase space. We can thus choose the

* pedro.fernandes_tavares@maxiv.lu.se

ISBN: 978-3-95450-208-0 doi:10.18429/JACoW-IPAC2019-TUYPLM3

optical parameters in the achromat to achieve linearisation without needing a harmonic cavity for this purpose. A sextupole is used in the centre of each achromat to minimize the second order dispersion at the end of the linac. These sextupoles are also used to tweak the linearisation through the bunch compressor. The R56 of the achromats is fixed and the compression is varied using the RF phase in the linac.

Bunch Length Measurements

Bunch length measurements have been performed while compressing only in bunch compressor 1 (BC1) and using bunch compressor 2 (BC2) as a streak camera. We then go off-crest in the main linac to create a correlated energy spread and look at the beam in a dispersive section in BC2. Using this method, a bunch length of 16 fs RMS was recorded (Figure 1). We did not have the resolution to measure anything shorter. Using the same method we have also been able to test the effectiveness of the sextupole linearization of longitudinal phase space (Figure 2). In [29], a measurement of the caustic nature of electron trajectories in the MAX IV bunch compressors is presented.

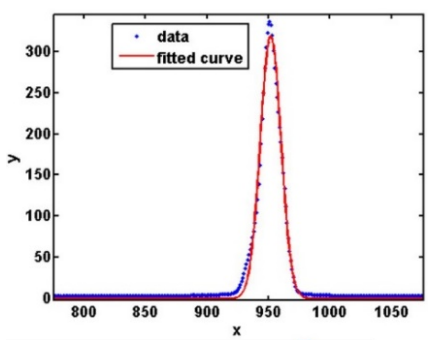

Figure 1: Bunch length measurement.

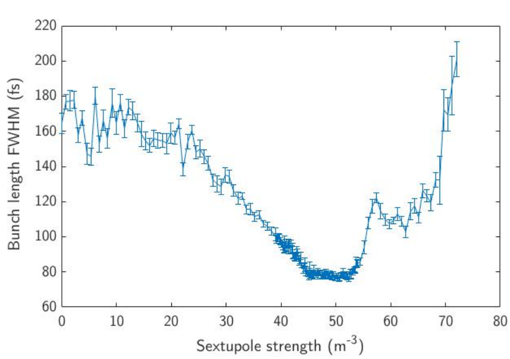

Figure 2: Bunch length as a function of sextupole strength in bunch compressor.

An alternative method to characterize electron bunch length, develop at the Cockroft Institute, based on THz imaging of coherent transition radiation has also been tested and after BC2 [31].

In order to improve both resolution and accuracy of the longitudinal bunch measurements a transverse deflecting cavity (TDC) is needed. Placing this TDC after the second compressor will ensure that we can measure the longitudinal phase space after both compressors (Figure 3).

TDC RF and Mechanical Design

Despite the fact that X and C-band structures offer higher deflecting gradients, the MAX IV TDC structures will operate at S-band (2.9985 GHz). This makes it possible to feed the structures with the same type of modulator and 37 MW klystrons as in the main MAX IV linac. By using a single RF station with a SLED system and two 3-m long TDC structures, a total integrated deflecting voltage of approximately 120 MV can be achieved.

The RF design [14] of the structures aims at maximum integrated deflecting voltage, while keeping surface fields and currents at a minimum. Each structure consists of two coupler cells and 89 regular cells, with a cell-to-cell phase advance of -2π/3. In order to change the polarization of the deflecting fields, the coupler cells are fed with two waveguides, as illustrated in Figure 4. To verify the RF concept, a 9-cell prototype was constructed and successfully tested in early 2019.

The coupler cells are brazed, while the regular cells are clamped together. The vacuum seal between the regular cells is achieved by using copper gaskets, as described in [15]. Installation of the structure is planned for autumn 2019-Spring 2020.

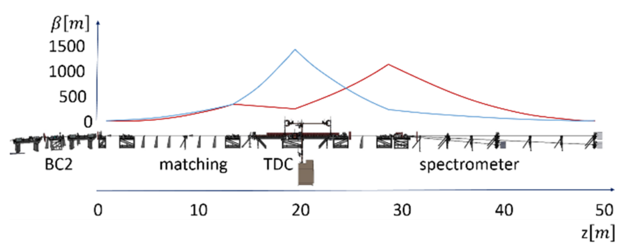

Figure 3: The TDC setup is installed in the SPF, following a new branch in BC2. The new BC2 branch can be turned on and off to either send the electron beam towards the TDC (new BC2 branch on) or towards the Femtomax beamline. The upper part shows the beta function along the set-up, horizontal in blue and vertical in red.

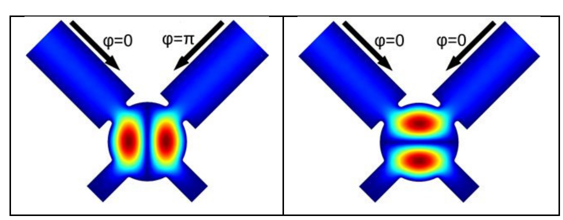

Figure 4: Electric field amplitude in the coupler cell when deflecting the beam in the horizontal plane (left), and in the vertical plane (right). φ is the relative phase of the incoming RF signal.

ISBN: 978-3-95450-208-0 doi:10.18429/JACoW-IPAC2019-TUYPLM3

1.5 GeV RING

ID Compensation

Early during the project phase it was expected that only global compensation of ID gap and phase changes, i.e. restoring the machine working point, would be required. Local matching of the optics was deemed not needed given what was known regarding the planned insertion devices [1], which led to all gradient magnets being connected in series within their respective families. Optics studies were done for local compensation though, as a strong device was expected to be installed at the identical SOLARIS machine [16].

Changing plans at MAX IV Laboratory led to the first insertion devices for the 1.5 GeV ring to be relatively strong devices, the epu95.2 for the FinEstBeaMS beamline and the epu84 for the BLOCH beamline. Optics studies [17] showed local compensation would now be required, in particular for epu95.2. An upgrade project is now ongoing, with the aim of breaking up the global circuits to cope with a significant number of insertion devices [18] enabling the correction scheme described in [17]. The SQFO combined sextupole-quadrupole magnets flanking an ID straight will be connected in series but with their own unique power supply. The SXCOSKW skew quadrupole magnets (implemented as trim coils in sextupole magnets), as well as the DIPC pole-face strips, will be broken up in a similar fashion, providing the required knobs to match the beta functions locally, including coupling.

The originally envisioned global compensation has in the meantime been implemented via a TANGO-based tune feedback. The transverse Bunch-By-Bunch (BBB) feedback system provides online tune readings, based on which adjustments of the global SQFO and DIPC gradient circuits can be calculated. Hence it is a 2x2 Multiple-Input-Multiple-Output (MIMO) system that should be controlled, which is done with a P-controller along with a linear plant model consisting of a tune response matrix valid at the nominal working point. The feedback operates at 0.33 Hz, preventing the working point from drifting, although, as shown in Figure 5, it is not capable of preventing transient tune shifts of 0.01 when epu95.2 moves while close to minimum gap. At the current working point of ν_x = 0.285, ν_y = 0.125 and with the current gap and phase movement speed this does not constitute an issue.

Non-Linear Dynamics - TRIBS

The use of Transverse Resonance Island Buckets (TRIBs) has been proposed and successfully implemented at BESSY [19] as a means to provide pseudo-single bunch operation. Following successful first tests of TRIBs optics performed on the MAX IV 3 GeV storage ring in collaboration with the BESSY accelerator physics team, the implementation of TRIBs was also tested in the 1.5 GeV ring for which there is a specific demand from the science community for timing modes.

TRIBs were generated (Figure 6) by operating the machine at zero horizontal chromaticity and near the horizontal third-order resonance. In order to populate the islands for one selected RF bucket, the beam was excited at the central tune frequency (0.3343,) with the bunch-by-bunch feedback system. When the bunch-by-bunch drive was turned off, the charge in the islands slowly diffused back to the core of the beam, with a time constant of approximately 10 minutes. By exciting the beam at the island tune, the island bunch could be depopulated without any loss of beam current. The experiments were performed at 3 mA beam current with no loss of beam lifetime or injection efficiency.

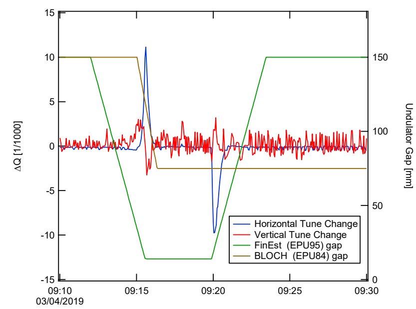

Figure 5: Residual transverse tune variations in the1.5 GeV ring as a result of closing of undulator gaps with global tune feedback ON.

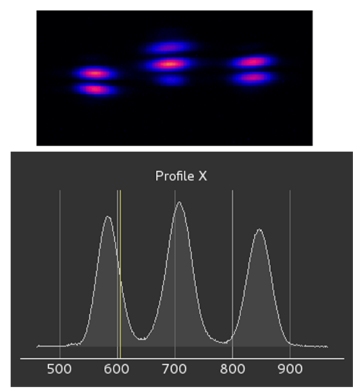

Figure 6: Horizontal TRIBs as observed at the MAX IV 1.5 GeV storage ring diagnostic beamline. The light from the islands is a projection of the phase space density distribution onto the horizontal axis.

3.0 GeV RING

Fast Orbit Feedback

The FOFB design in the 3 GeV ring calls for two sets of corrector magnets. This resulted from a vacuum system largely made of Cu which severely restricts the bandwidth of the 380 standard iron-core corrector magnets. An extra set of weak but fast window-frame magnets thus had to be installed over the few available stainless steel sections. The intent is to periodically off-load the fast corrector magnets using the stronger, slower, and more numerous standard correctors. The scheme is described in [20] and is based on what has been implemented at Synchrotron SOLEIL [21].

While the FOFB system for the 3 GeV ring was planned for already during the MAX IV project design phase [20],

ISBN: 978-3-95450-208-0 doi:10.18429/JACoW-IPAC2019-TUYPLM3

due to the very low ambient noise level [10] it has not so far been required for managing the orbit noise. Furthermore the insertion device orbit distortions have been manageable via a combination of dedicated ID orbit corrector coils in a feed-forward correction scheme, the Slow Orbit Feedback working at a relatively high rate of 3 Hz, and reduction of ID gap and phase movement speed to match the monochromator. As more hardware and insertion devices have been and are scheduled to be installed, the potential sources of orbit distortions are increasing, as is the sensitivity of the beamlines raising the priority of the FOFB.

All FOFB system hardware has been, with the sole exception of the final fast corrector power supplies, installed. A test setup with 8 prototype power supply units was installed in late December 2018 around the NanoMAX beamline ID. This test setup is currently being used for system tests of the FOFB installation and validating the power supply specifications ahead of procurement of the full system. The Global Data Exchange (GDX) and FOFB application [22] are currently being tested.

Off-Energy Orbit Response Matrix

The derivative of the beta functions with respect to momentum are linear with respect to sextupole field component [23,24]. The orbit response to a dipole kick at an off-nominal energy is approximately linearly dependent on the sextupole fields in the lattice so that the chromatic changes of measured orbit response matrix can be used to derive estimated sextupole strengths in a similar way to the fitting of quadrupole strengths through the well-known LOCO algorithm [25]. In order to test this method´s resolution, a set of five sextupole errors were introduced to the MAX IV 3 GeV storage ring, by reducing the current in the coils of five sextupole family circuits by 20%,10%, 5%, and 2% respectively. By analysing the measured off-Energy Orbit Response Matrix (OEORM) before and after introducing the errors it was possible to resolve all but the 2% error. Next, by iteratively applying corrections from the measured OEORM the chromaticity of the ring was corrected to the nominal value (+1/+1). The new sextupole settings found using this procedure are currently in use as the production optics in the MAX IV 3 GeV storage ring. They have resulted in an increase of injection rate at design tunes (0.2000/0.2800) from ~3 mA/min to ~18 mA/min. No loss of beam lifetime has been observed at the new settings

Effective Impedance Measurements

The broadband impedance of the MAX IV 3 GeV ring has been measured and is documented in [10], where the only component that is not estimated is the imaginary part of the longitudinal impedance. This was because it was not possible to separate the contributions of intrabeam scattering (IBS) and potential-well distortion (PWD) to the lengthening of bunches with current. With the completion of two diagnostic beamlines, a measurement of the energy-spread, which is not directly influenced by PWD, is now available.

The estimated normalised effective impedance $(Z_{\parallel}/n)_{\text{eff}}$, based on the impedance model of the 3 GeV ring, is 0.16 Ω. This includes the geometric contribution, which accounts for 46% of the total, estimated using GdfidL [27] and the resistive-wall impedance of the NEG-coated copper chamber estimated using Impedance-Wake2D [28]. The estimated effect of the NEG coating is an increase in the total normalised effective impedance of 48%. Using the above estimate, along with zero-current values of 330 pm rad and 6 pm rad for the horizontal and vertical emittances respectively and 40 ps for the natural bunch length, a self-consistent IBS calculation using ZAP gives a value of 0.93×10-3 for the energy spread of a 4 mA bunch. This is a significant increase from the natural energy spread of 0.79×10-3.

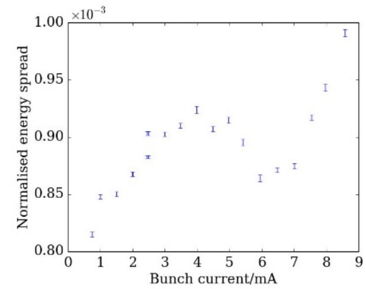

Figure 7: Measured energy spread as a function of single bunch current.

Figure 7 shows the normalised energy spread measured over a range of single-bunch currents using the aforementioned beamlines. For the points below 2.5 mA, four bunches of equal charge were injected into the ring to obtain sufficient image intensity. Above a threshold of 6 mA, a sextupole head-tail instability develops, resulting in an increase in energy spread. The energy spread at 4 mA bunch current is in good agreement with the prediction, although a full quantitative analysis to obtain more precise estimates and to fully explain the trend, including the decrease in energy spread above 5 mA bunch current, is underway.

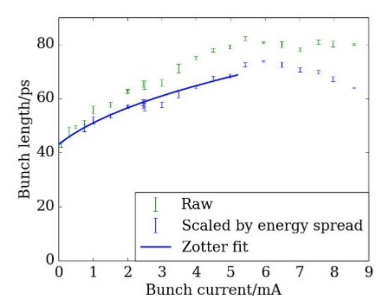

Figure 8: Bunch length as a function of current, with and without scaling by the measured energy spreads shown in Figure 7.

Figure 8 shows the bunch length measured using an optical sampling oscilloscope (OSO) as a function of bunch current before and after scaling by the energy spread measured at the same current. Such a scaling is employed to isolate the effect of PWD. A Zotter curve [26] is fitted to the scaled results up to a single-bunch current of 5 mA. This point was chosen since this is where the energy spread

ISBN: 978-3-95450-208-0 doi:10.18429/JACoW-IPAC2019-TUYPLM3

starts to decrease and a departure from the expected trend is seen. From the fit, the normalised effective impedance can be estimated. Due to hitherto unidentified systematic errors, the value obtained varies a lot between measurements carried out on different days. However, it is clear that the effect of IBS is very significant, leading to a reduction in the estimate from a value in the range of 0.7-1.0 Ω to one in the range of 0.2-0.5 Ω. Possible sources of systematic uncertainty include the different timescales over which the various instruments average and thermal drifts in the optical beamline.

Vacuum System

The vacuum performance can be measured by the average pressure reduction and by the increase of the total beam lifetime with the accumulated beam dose (Figure 9). After each shutdown, there is an increase in the normalized average pressure followed by a fast recovery with further vacuum conditioning of around 18-30 Ah depending on the scale of the interventions performed. The increase in the normalized beam lifetime I.τ vs. accumulated beam dose (Figure 9) is an indication of the beam cleaning effect and vacuum conditioning. Typical beam lifetime during delivery at 250 mA is 12-15 h.

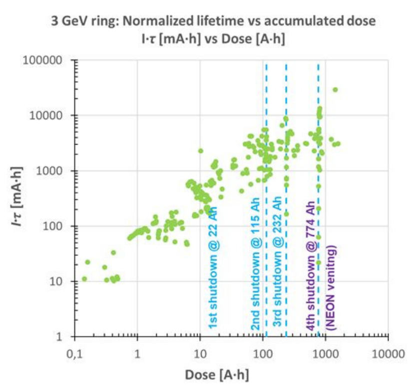

Figure 9: Normalized beam lifetime (mAh) vs accumulated beam dose (Ah).

A neon venting procedure first developed at CERN for activated NEG coated vacuum chambers was successfully tested at the MAX IV in June 2018. The procedure avoids saturating the NEG coating, thus eliminating the need of baking and re-activation of the film. The normalized average pressure rise before the intervention (venting of two achromats for chamber replacement) was 9.3·10-13 mbar/mA, just after the intervention (after 1 Ah) this value increased to 2.4·10-11 mbar/mA, and after 18 Ah of beam conditioning this normalized average pressure rise reduced significantly to 1.2·10-12 mbar/mA. The lifetime before the intervention was ranging between 3-5 Ah, just after the intervention (after 1 Ah) this value reduced to 1.2 Ah, and after 18 Ah of beam conditioning the lifetime increased significantly back to the original value from before intervention (3.8 Ah). The implementation of neon venting as the procedure to be followed for vacuum interventions that involve replacing vacuum chambers or components in the 3 GeV ring reduced significantly needed time and risks.

ACCELERATOR OPERATIONS

Throughout 2018, the MAX-IV accelerators showed a strong shift from the commissioning phase of the project lifecycle towards the delivery stage. Operator coverage has increased from 16 hours per day at the end of 2017, to full, three-shift, 24/7 staffing. A standard week consists of 142 hours of delivery to beamlines, leaving a 26 hour period for maintenance and start-up activities. Operational statistics for 2018, the second year of regular user operations, are shown in Table 1.

At present, both the 3 GeV and 1.5 GeV rings have a nominal stored current of 250 mA, with top-up injections every 30 minutes. These top-up shots briefly interrupt beam to the Short Pulse Facility (SPF), which typically delivers compressed bunches of ~100 pC at 2 Hz for user experiments. In total, as of April 2019, 10 beamlines are served by the MAX-IV accelerators – 5 in the 3 GeV ring, 4 in the 1.5 GeV ring, and 1 in the SPF.

Table 1: 2018 Delivery Figures of Merit for the MAX-IV Accelerators

	3 GeV Ring	**1.5 GeV Ring**	**SPF**
Delivery [hr]	4068	2953	2467
Avail. [%]	96.2	96.7	95.4
MTBF [hr]	34.5	59.6	32.7
MTTR [hr]	1.3	1.9	1.5

CONCLUSIONS

The MAX IV facility is now in full operation providing reliable high brightness beams to the Swedish, Nordic and international scientific communities. As the first example of a multi-bend achromat, ultra-low emittance machine, the MAX IV 3 GeV ring in particular also serves as a relevant benchmark for a number of design strategies that are common to several new projects aiming at even higher brightness and that are currently under way all over the globe. Future perspectives at MAX IV include a soft X-Ray Free-electron laser based driven by the 3 GeV injector linac.

REFERENCES

[1] MAX IV (2010). MAX IV Detailed Design Report,

[2] P.F.Tavares *et al.*, "The MAX IV Storage Ring Project", J. Synchrotron Rad. (2014). 21, 862–877.

[3] M.Johansson *et al.*, "Magnet Design for a Low-Emittance Storage Ring", J. Synchrotron Rad. (2014) 21, 884–903.

[4] Al-Dmour *et al.*, "Diffraction Limited Storage Rig Vacuum Technology", J. Synchrotron Rad. (2014) 21, 878–883.

[5] Å.Andersson *et al.*, "The 100 MHz RF system for the MAX IV storage rings", in *Proc. IPAC11*, p.193-195.

[6] P.F.Tavares *et al.*, "Equilibrium bunch density distribution with passive harmonic cavities in a storage ring", Phys. Rev AB, 17, 064401 (2014).

[7] M.Eriksson *et al.*, "Commissioning of the MAX IV Light Source", IPAC 16, p. 11.

[8] P.F.Tavares *et al.*, "Commissioning of the MAX IV Light Source", NAPAC 16, p. 439.

ISBN: 978-3-95450-208-0 doi:10.18429/JACoW-IPAC2019-TUYPLM3

[9] S.C.Leemann *et al.,* "First optics and beam dynamics studies on the MAX IV 3 GeV storage ring", NIMA Vol. 883, 2018, p. 33-47.

[10] P.F.Tavares *et al.*, "Commissioning and first year operational results of the MAX IV Light Source", J. Synchrotron Rad. (2018). 25, p. 1291–1316.

[11] S.Thorin *et al,* "The MAX IV Linac". No. LINAC-2014-TUIOA03. 2014.

[12] H.Enquist *et al.*, "FemtoMAX–an X-ray beamline for structural dynamics at the short-pulse facility of MAX IV." Journal of synchrotron radiation 25.2 (2018): 570-579.

[13] S. Thorin *et al.*, "Bunch Compression by Linearising Achromats for the MAX IV Injector" WEPB34, FEL2010.

[14] D.Olsson *et al.*, "Transverse RF Deflecting Structures For The MAX IV Linac", in *Proc. IPAC18*, Vancouver, Canada, p.3684.

[15] D.Alesini *et al.*, "Design, realization, and high power test of high gradient, high repetition rate brazing-free S-band photogun", Phys.Rev.Acc.Beams 21, 112001 (2018).

[16] A. I. Wawrzyniak *et al*, "Solaris Storage Ring Lattice Optimisation with Strong Insertion Devices", Proceedings of IPAC2012, New Orleans, Louisiana, USA.

[17] S. C. Leemann *et al.*, "Impact of Insertion Devices On The Max IV Storage Rings", in *Proc. of IPAC2015*, Richmond, VA, USA.

[18] H. Tarawneh *et al.*, "First Commissioning Results of Phase I Insertion Devices at MAX IV Laboratory", AIP Conference Proceedings 2054, 030023 (2019).

[19] P. Goslawski *et al,* "Status of Transverse Resonance Island Buckets as Bunch Separation Scheme, ", *in Proc. of IPAC2017*, Copenhagen, Denmark, p. 3019.

[20] M. Sjöström *et al.,* "Orbit Feedback System for the MAX IV 3 GeV Storage Ring," *in Proc. of IPAC2011*, San Sebastían, Spain

[21] N. Hubert *et al*., "Global orbit feedback systems down to DC using fast and slow correctors", DIPAC'09, Basel, Switzerland, May 2009, MOOC01.

[22] P. Leban *et al*., "Fast Orbit Feedback Application at MAX IV and SOLARIS Storage Rings", *in Proc IPAC2014*, Dresden, Germany.

[23] N. Carmignani, "Sextupole Calibrations via Measurements of Off-Energy Orbit Response Matrix and High Order Dispersion", presented at the 25th European Synchrotron Light Source Workshop (ESLS'17), Dortmund, Germany, Nov. 2017.

[24] H. Wiedemann, "Hamiltonian Nonlinear Beam Dynamics", in Particle Accelerator Physics, Springer, 2007, pp. 503-534.

[25] J.Safranek, "Experimental determination of storage ring optics using orbit response measurements", NIM A, Vol 388, p.27-36 (1997).

[26] B.Zotter, "Potential Well Bunch Lengthening", CERN-SPS-81-14-DI. 1981.

[27] W. Bruns, "The GdfidL Electromagnetic Field Simulator", www.gdfidl.de, 2015.

[28] N. Mounet, "ImpedanceWake2D", https://impedance.web.cern.ch/impedance/Codes/ImpedanceWake2D/user_manual, 2011.

[29] T. K. Charles, et al., "First Experimental Measurements of the Caustic Nature of Electron Trajectories in Bunch Compressors", *presented at the 10th Int. Particle Accelerator Conf. (IPAC'19)*, Melbourne, Australia, May 2019, paper WEYYPLS2, this conference.

[30] Z.D.Farkas *et al.*, "Recent Progress on SLED, The SLAC Energydoubler", IEEE Transactions on Nuclear Science, VoLNS-22, No.3, June 1975.

[31] Joseph Wolfenden *et al*., "Coherent Transition Radiation Spatial Imaging as a Bunch Length Monitor", these proceedings.